

Fracture in spruce: experiment and numerical analysis by linear and non linear fracture mechanics

L. Daudeville

Abstract That paper first presents a simplified Damage Mechanics (DM) model for the simulation of fracture in wood. All damage phenomena are assumed to occur on a surface (or a line in a 2D problem). Then test results of mode I fracture in spruce and fir are given. The size effect is investigated. Linear Elastic Fracture Mechanics (LEFM) and DM are compared for a simulation of three point bending tests, classically used for the determination of the fracture energy (G_f) in tension perpendicular to grain. The study of the observed size effect gives the range of applicability of LEFM. The critical energy release rate (G_c) and the fracture energy (Y_f) that are energy parameters of LEFM and DM respectively, are identified for small specimens and compared with the experimentally dissipated energy to fracture the specimen (G_f). Load-displacement curves are correctly predicted with both methods. G_f can be considered as a material parameter and it is verified that a non-linear approach is necessary for the simulation of fracture of small specimens.

Bruchverhalten von Fichtenholz: Experimente und numerische Analyse mittels linearer und nicht-linearer Bruchmechanik

Die Arbeit stellt zunächst ein vereinfachtes Modell der Schadensmechanik (DM) zur Simulation des Bruchverhaltens vor. Für alle Schädigungen wird angenommen, daß sie an der Oberfläche stattfinden (bzw. in einer Linie bei einem 2D-Problem). Danach werden Testergebnisse des Bruchverhaltens in Mode I für Fichten- und Tannenholz beschrieben. Der Einfluß der Probengröße wird dabei untersucht. Lineare elastische Bruchmechanik (LEFM) und DM werden verglichen für den Fall einer Drei-Punkt-Biegeprüfung, die üblicherweise zur Bestimmung der Bruchenergie (G_f) senkrecht zur Faser herangezogen wird. Der Einfluß der Probengröße bestimmt den Bereich der Anwendbarkeit der LEFM. Die kritische freigesetzte Energie (G_c) und die Bruchenergie (Y_f), beides Parameter der LEFM, werden für jede Probe bestimmt und mit der

experimentell freigesetzten Energie beim Bruch (G_f) verglichen. Die Verformung unter Belastung wird mit beiden Methoden korrekt beschrieben. G_f kann als Materialkonstante angesehen werden. Es wird gezeigt, daß zum Beschreiben des Bruchverhaltens kleiner Proben ein nichtlinearer Ansatz notwendig ist.

1 Introduction

Normally, timber structures are designed with the intent of avoiding failure modes associated with crack growth parallel to the grain. Therefore, the study of cracking, which may be responsible for structural timber failure in a large number of cases, is necessary to evaluate the load-bearing capacity of a structure or of a sub-structure (e.g. notched beams or mechanical joints).

In classical Linear Elastic Fracture Mechanics (LEFM) (Griffith, 1920), a theory which is commonly used for the fracture analysis of metals or brittle materials such as ceramics, all damage phenomena are assumed to be concentrated at the crack tip. Non Linear Fracture Mechanics (NLFM) introduces the notion of a planar process zone where cohesive stresses are assumed to occur (Hillerborg et al., 1976; Bazant and Kazemi, 1990; Jenq and Shah, 1985; Nallathambi and Karihaloo, 1986) for concrete and (Gustafsson, 1988; Boström, 1988) for wood.

A simplified approach based upon Damage Mechanics (DM) for the analysis of cracking is presented. NLFM and DM have been developed to treat the problem of fracture in materials that exhibit a softening behavior (i.e. quasi-brittle materials). In such materials, fracture is preceded by localization phenomena. In the proposed approach, damage is assumed to occur on a surface (or on a line in a 2D problem) called an interface. The interface model relates tractions to relative displacement jumps in the localized zone. Damage is described by means of the relative variations of stiffness.

An important limitation of LEFM is the necessity of assuming the existence of a crack. Both NLFM and DM concepts can be applied to treat the problem of crack initiation in originally uncracked structures. In this paper the problem of propagation of an already cracked area is studied.

NLFM has been essentially applied to the problem of fracture in concrete. In such an isotropic material, the first mode of fracture (tension) is predominant. Because of the orthotropic behavior of wood, the crack propagates along the grain under pure or mixed mode conditions. In the present study, joint elements are used in a Finite Element

L. Daudeville
Laboratoire de Mécanique et Technologie
ENS de Cachan/CNRS/Université Pierre et Marie Curie
61 avenue du Président Wilson, F-94235 Cachan Cedex, France

The author thanks Prof. Yasumura from Shizuoka University for his advice, Prof. Ohta from University of Tokyo for providing specimens and his help during experiments and Dr. Lanvin from CTBA Paris for giving specimens and advice.

(FE) scheme, in association with the DM model for the analysis of cracking along an expected crack path. Such techniques were used for different applications in civil engineering (Ngo and Scordelis, 1967; Hohberg and Bachmann, 1988; Gens et al., 1988; Rots and Schellekens, 1990; Garcia-Alvarez et al., 1994).

The proposed damage model and fracture mechanics have the same kind of application and a link between the two approaches is possible in terms of fracture energy.

The so-called “size effect” is defined through a comparison of geometrically similar structures of different sizes. Discussions are given in (Bazant, 1984) for concrete or in (Aicher, 1992; Aicher et al., 1993) for wood. In the analysis of this phenomenon, one may separate size-effect into a “volume effect” which is due to the existence of defects in the material and a “structural effect” which is the direct effect of the size on the response of cracked structures.

The process zone is a relatively important region for small specimens but is negligible for large specimens. In the former case, the process zone influence produces a size effect on the nominal strength that does not vary as the inverse square root of the characteristic size ($h^{-0.5}$) like in LEM (Bazant, 1984). DM and NLFM take into account the process zone influence for small specimens.

An experimental program was performed for the mode I fracture analysis of spruce and fir species. The three point bending (TPB) test proposed at CIB-W18 (Larsen and Gustafsson, 1989) was first carried out for the determination of fracture energy with respect to the wood orientation (denoted RL and TL in the literature) and for a fixed beam depth ($h = 45$ mm) and width ($b = 45$ mm). The study of the beam depth influence on the nominal stress ($h = 45, 67, 100$ mm), with a given wood orientation (TL) and a fixed beam width ($b = 45$ mm), shows that LEM concepts are not valid for the smallest beams as demonstrated in (Aicher et al., 1993). Another important result is that the fracture energy (G_f) does not depend on the specimen size for the considered specimens.

In order to verify these experimental observations, TPB tests with the smallest size were first simulated by means of LEM. Some typical tests were chosen. It may be assumed that proposed conclusions would be the same by simulating other tests.

The FE method is used for the analysis of the crack propagation. The critical energy release rate (G_c), normally a material property, here a theoretical quantity, is determined from the maximum load (onset of propagation of the initial crack).

In a second step, the TPB test was analyzed by the FE method with the DM model. The only determined parameter is the fracture energy per unit cracked area (Y_f) which is a material parameter of the modeling and which depends on the wood orientation. Y_f was determined from the maximum load.

Load-displacement curves are correctly described with both LEM and DM. As expected, the identified critical energy release rate (G_c) is different from the experimental fracture energy (G_f) but the fracture energy of the DM model (Y_f) is close to G_f .

The previous result confirms that the fracture energy is the parameter that governs fracture propagation and that

fracture energy obtained with the CIB-W18 TPB test can be considered as a material parameter for the analysis of fracture.

2 Experiments

2.1 Presentation

An experimental program has been carried out at CTBA Paris and University of Tokyo for the determination of the fracture energy in tension perpendicular to grain of spruce and fir species. According to RILEM and CIB-W18 recommendations (Larsen and Gustafsson, 1989), TPB tests were performed in order to obtain a stable crack extension in the longitudinal-tangential and longitudinal-radial growth planes, denoted RL and TL respectively, from an initial notch to the complete separation of both crack faces (Fig. 1).

The mean density of wood is 440 kg/m^3 . Specimens were conditioned at $20 \pm 2 \text{ }^\circ\text{C}$ and $65 \pm 5\% \text{ RH}$. All the specimens have the same width ($b = 45$ mm), the depth (h) varies between 45 and 100 mm.

The stroke speed is chosen proportional to the depth (h) in order to prescribe a constant strain rate. For smallest specimens ($h = 45$ mm), the head speed was chosen equal to 0.5 mm/min . in order to obtain approximately the same strain rate as in the Larsen and Gustafsson tests (1990).

A classical parameter of fracture for quasibrittle materials is the fracture energy G_f . It is the dissipated energy per unit crack area. It is experimentally obtained by analyzing the whole dissipated energy in a specimen. The fracture energy is (Larsen and Gustafsson, 1989):

$$G_f = \frac{W + m g u_0}{h_0 b} \quad (1)$$

W is the area under the load deflection curve by considering an “equivalent force” $P_{\text{eq}} = P - m g/2$ to take into account the work due to the weight, u_0 is the de-

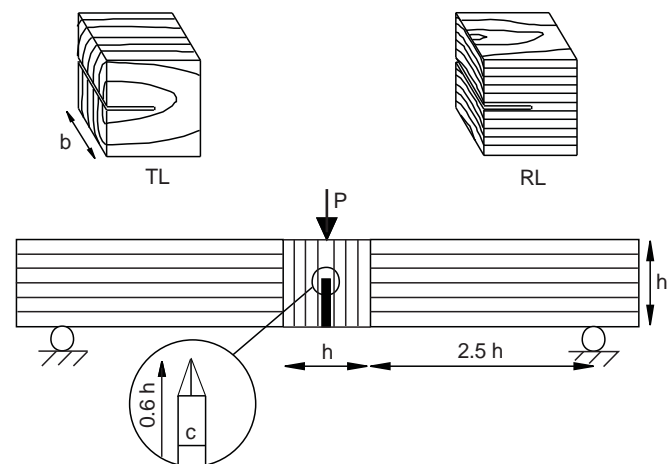


Fig. 1. Three point bending test (Larsen and Gustafsson 1989)
Bild 1. Drei-Punkt-Biegeprüfung nach Larsen und Gustafsson (1989)

flexion at failure, m is the mass of the beam, g is the gravity acceleration, b is the beam width and h_0 is the ligament length.

2.2 Preliminary numerical results

The next section will discuss the numerical simulation of these tests with both LEFM and DM models. Preliminary results are given for the discussion of tests. Figure 2 gives the theoretical influence of the notch shape on the stability of the load-deflection response computed by means of LEFM. A thin notch ($c = 1$ mm) finalized with a 1 mm razor blade (Fig. 1) is better than a V-notch ($c = 3$ mm).

Figure 3 shows the theoretical influence of the initial crack length on the load-displacement response computed by means of DM. An initial crack length, equal to 60% of the beam depth (h), ensures a stable response. This initial crack length was also used by Aicher (1992).

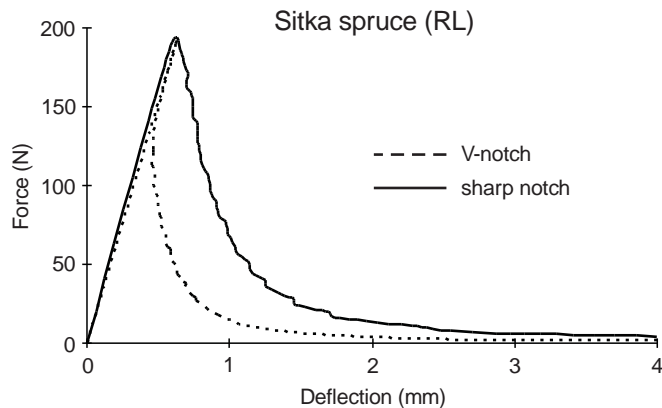


Fig. 2. Theoretical influence of the notch shape on the stability of the load-deflection response computed by means of LEFM
Bild 2. Theoretischer Einfluß der Nutform auf die Stabilität des Verhaltens unter Belastung und Entlastung entsprechend der linearen elastischen Bruchmechanik (LEFM)

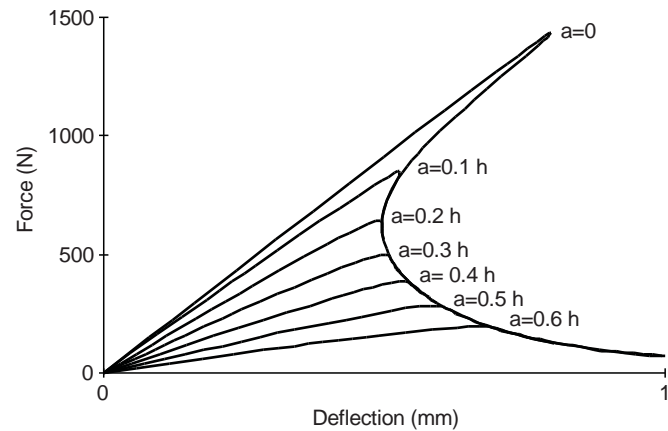


Fig. 3. Theoretical influence of the initial crack length computed by means of DM

Bild 3. Theoretischer Einfluß der anfänglichen Rißlänge, berechnet mittels "Damage Mechanics" (DM)

2.3 Results

Table 1 gives the fracture energies with respect to the growth plane and to the specimen depth (h). The mean fracture energy value of white wood for the lower depth ($h = 45$ mm, 107 specimens, spruce and fir, any orientation), close to 200 Nm/m^2 , is lower than the value obtained by Larsen and Gustafsson (1990). Note that the number of tests presented in the previous paper is low for the concerned density and beam depth. The presented result for spruce and for the orientation RL ($h = 45$ mm) is close to the fracture energy value found in (Aicher, 1992) with quite the same dimension ($b = 44$ mm, $h = 10\text{--}320$ mm).

2.3.1 Size effect

The influence of the specimen dimensions was also investigated for spruce and fir in the TL orientation only. In order to analyze the structural effect and not the volume effect, specimens were 2D-similar: only the depth was modified ($h = 45, 67, 100$ mm) but not the width ($b = 45$ mm).

Table 1. Fracture energy (G_f) of spruce and fir specimens with constant width ($b = 45$ mm) versus the specimen depth (h). Tests 1 and 2 were performed at Paris, tests 3 and 4 at University of Tokyo. Tests 1, 2 and 4 use French wood. Tests 3 use north American spruce. Nb denotes the number of tests and cv the coefficient of variation (%)

Tabelle 1. Bruchenergie (G_f) von Fichten- und Tannenproben konstanter Breite ($b = 45$ mm) in Abhängigkeit von der Probenhöhe (h). Tests 1 und 2 wurden in Paris durchgeführt; Tests 3 und 4 an der Universität in Tokyo. Tests 1, 2 und 4 verwendeten französische Holzproben, Test 3 nordamerikanische Fichte. Nb bezeichnet die Anzahl der Prüfungen und cv den Variationskoeffizienten (%)

| Species | h (mm) | Orient. | Mean (Nm/m^2) | Min (Nm/m^2) | Max (Nm/m^2) | Nb (cv %) |
|-----------------------------|----------|---------|--------------------------|-------------------------|-------------------------|-----------|
| Spruce ¹ | 45 | RL | 220 | 159 | 345 | 32 (19) |
| (<i>Picea excelsa</i>) | 45 | TL | 160 | 100 | 247 | 10 (29) |
| Fir ² | 45 | RL | 210 | 126 | 367 | 35 (26) |
| (<i>Abies pectinata</i>) | 45 | TL | 157 | 97 | 236 | 5 (37) |
| Sitka Spruce ³ | 45 | RL | 220 | 157 | 248 | 5 (16) |
| (<i>Picea sitchensis</i>) | 45 | TL | 164 | 136 | 196 | 5 (16) |
| Spruce and Fir ⁴ | 45 | RL | 251 | 184 | 371 | 5 (31) |
| (not distinguished) | 45 | TL | 157 | 133 | 214 | 10 (15) |
| Spruce and Fir ⁴ | 67 | TL | 160 | 115 | 209 | 9 (19) |
| Spruce and Fir ⁴ | 100 | TL | 159 | 112 | 279 | 8 (34) |

The nominal stress (σ_N) is defined as:

$$\sigma_N = \frac{P + \frac{5mg}{12}}{bh} \quad (2)$$

with P is the maximum force and m the mass of the beam. According to LEFM, σ_N varies as $h^{-0.5}$. In Fig. 4 are plotted G_f and $\ln(\sigma_N)$ versus $\ln(h)$. This figure shows that the LEFM nominal strength prediction is correct for the two largest specimen sizes but not for the 45 mm one due to the influence of the process zone on the whole fracture process of the specimen. It is possible to define a brittleness number for the discussion of LEFM applicability (Bazant and Pfeiffer, 1987).

Table 1 and Fig. 4 show that the size effect seems to be insignificant for fracture energy. Larsen and Gustafsson (1990) noticed a slight size effect but these authors increased proportionally both the beam thickness and depth h ($h = 40-160$ mm). The size effect of the previous authors may be due to the increase of defects as the thickness increases.

Aicher (1993) obtained the same conclusions as the ones presented here for specimen depths (h) varying from 10 to 320 mm for a RL orientation and a constant beam width ($b = 44$ mm).

3 Modeling of localized fracture with damage mechanics

Damage phenomena are assumed to be concentrated on a zero-thickness interface. Interface modeling allows a study of crack propagation under pure or mixed mode conditions.

The main features and assumptions of the damage model are: Damage is described through the damage variables d_1 and d_2 which are the relative stiffness decreases; further there is no damage under compression (unilateral effect) and there are no irreversible displacement discontinuities. During the elastic stage of the loading process, no significant relative displacement occurs.

The interface Γ connects the two parts of a solid Ω^+ and Ω^- (Fig. 5).

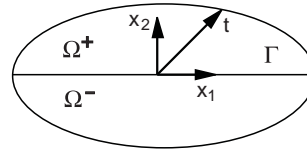


Fig. 5. Local directions of joint element (x_1 is the grain direction)
Bild 5. Lokale Koordinaten (Richtungen) eines Verbundungselements (x_1 ist die Faserrichtung)

To simplify, let us consider a plane stress problem in the plane x_1x_2 (x_1 is a unit vector along the grain direction). The relative displacement vector $[u]$ at point P is ($[x]$ denotes the jump of the quantity x between the Ω^+ and Ω^- regions):

$$[u] = u^+ - u^- = [u_1]x_1 + [u_2]x_2 \quad \text{with } [u_2] \geq 0 \quad (3)$$

The traction vector is:

$$t = \sigma_{12}x_1 + \sigma_{22}x_2 = k_1(1 - d_1)[u_1]x_1 + k_2(1 - d_2)[u_2]x_2 \quad (4)$$

d_1 and d_2 are the respective damage indicators in mode II and I. The stiffnesses k_1 and k_2 have to be high to ensure continuity of displacement when there is no damage (penalty factors).

An example of a traction-relative displacement curve in mode I is given in Fig. 6.

The variables Yd_i ($i = 1, 2$) which are similar to the energy release rates introduced in Fracture Mechanics, are conjugated to d_i ($\langle x \rangle_+$ denotes the positive part of x):

$$Y_{d_1} = \frac{1}{2} \frac{\sigma_{12}^2}{k_1(1 - d_1)^2} \quad \text{and} \quad Y_{d_2} = \frac{1}{2} \frac{\langle \sigma_{22} \rangle_+^2}{k_2(1 - d_2)^2} \quad (5)$$

The damage evolution equations are relations between d_1 , d_2 and Y_{d_1} , Y_{d_2} . A particular choice of the damage evolution law is presented:

$$\underline{Y} = \sup_{\tau \leq t} (Y_{d_1} + \gamma Y_{d_2}) \quad (6)$$

where $\sup_{\tau \leq t} x$ is the maximum value of $x(\tau)$ with time τ between 0 and t . γ is a coupling factor between modes I and II and:

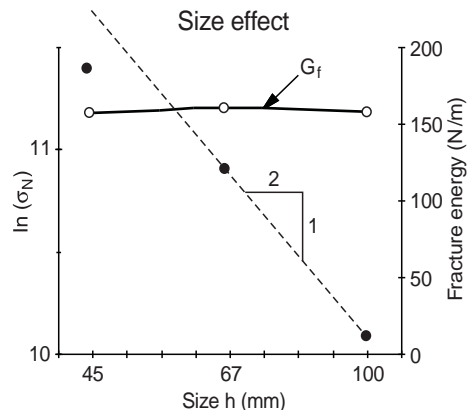


Fig. 4. Size effect on the nominal strength (σ_N) and the fracture energy (G_f) for a TL orientation

Bild 4. Einfluß der Probengröße auf die nominale Festigkeit (σ_N) und die Bruchenergie (G_f) für eine TL-Orientierung

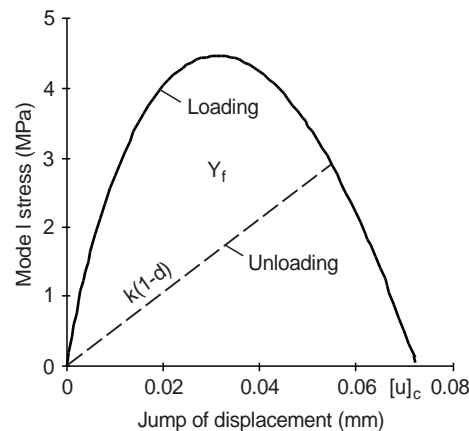


Fig. 6. Constitutive behavior in mode I
Bild 6. Verformungsverhalten in Mode I

$$d = d_1 = d_2 = w(\underline{Y}) = \left(\frac{\underline{Y}}{Y_f} \right)^n \quad \text{and} \quad d \leq 1 \quad (7)$$

Y_f and n are characteristic parameters of the damage evolution law of the interface. Y_f corresponds to a critical energy. These parameters can be identified by the analyze of fracture tests.

3.1 A link with Linear Elastic Fracture Mechanics

Interface models are introduced for the simulation of decohesion between two solids or between two parts of a solid. Classical fracture tests may be used for the identification of fracture models. A link between Damage Mechanics and Fracture Mechanics is presented (Allix et al., 1994).

Through fracture tests (Valentin et al., 1989) one can obtain the three inter-laminar fracture toughnesses G_{Ic} , G_{IIc} and G_{IIIc} relative to the modes I, II and III. G_{ic} values ($i = I, II, III$) are different because of the interface orthotropy. G_{ic} are defined in the framework of LEFM.

3.1.1 Analysis of fracture propagation

The dissipative phenomena are assumed to occur on the interface Γ only. Let us consider a steady state of fracture propagation. This means that during crack propagation the process-zone has a constant size and translates without modification. This distinction between the fracture onset and the steady state of propagation is classical for quasibrittle materials that exhibit a R-curve effect. Here, contrary to the critical energy release rate $G(a_0, P_u)$, defined at the onset of cracking for the ultimate load P_u and for the initial crack length a_0 , the critical energy release rate $G_c = G(a, P)$ defined for a steady state of fracture propagation, is considered. The latter quantity is hard to obtain experimentally because of the difficulty to measure the crack length (a) during the test.

Let us define the crack tip by $d = 1$. An equivalence of dissipated energies per unit cracked area gives:

$$G_c = G_I + G_{II} = \int_{d=0}^{d=1} Y_{d_2} \delta d + \int_{d=0}^{d=1} Y_{d_1} \delta d \quad (8)$$

A mixed mode of fracture is considered. The intrinsic toughnesses G_{Ic} and G_{IIc} have to be introduced. Let us define the ratio c such that:

$$c = \frac{Y_{d_1}}{Y_{d_2}} = \frac{G_{II}}{G_I} \quad \text{then} \quad G_c = \int_{d=0}^{d=1} (1 + c) Y_{d_2} \delta d \quad (9)$$

By considering the constitutive equations (6), (7), this becomes:

$$G_c = \frac{(1 + c) Y_f}{1 + \gamma c} \quad (10)$$

In particular, under pure modes of fracture:

$$G_{Ic} = Y_f; \quad G_{IIc} = \frac{Y_f}{\gamma} = \frac{G_{Ic}}{\gamma} \quad (11)$$

The previous equations give some relations between Fracture Mechanics and Damage Mechanics parameters.

Using (8)–(11), the criterion for fracture propagation under mixed mode conditions is:

$$\frac{G_I}{G_{Ic}} + \frac{G_{II}}{G_{IIc}} = 1 \quad (12)$$

The particular choice of the damage evolution (6), (7) is then justified: this kind of propagation criterion is classically proposed in the available analyses of fracture in orthotropic materials such as wood (Hunt and Croager, 1982; Lum and Foschi, 1988; Murphy, 1986; Patton-Mallory and Cramer, 1987; Triboulot et al., 1984; Valentin et al., 1991). The second term of Eq. (12) can be written with an exponent (generally equal to 2) as proposed by some authors (Wu, 1967; Mall et al., 1983). The proposed damage evolution law (6), (7) can be modified similarly.

Note that critical energy release rates are not sufficient data because they only give information about the area under the stress-displacement curves but not on their shapes.

3.1.2 Fracture energy

Now the fracture energy (G_f), dissipated during complete cracking of a specimen (e.g. in mode I), is considered. In the case of a perfectly brittle material, there is no process zone, thus transient and steady states of propagation are similar and then:

$$G_f = G_c \quad (13)$$

The previous result is still valid for quasibrittle materials, but only for large structures, in which the influence of the process zone can be neglected (Bazant, 1984). In the general case of quasibrittle materials and non-large structures, Eq. (13) does not hold.

3.2 Finite element strategies

The presented damage model was implemented in a FE code. Joint elements were used to model the decohesion between parts of the structure. Due to damage on interfaces, a instability point may appear. This critical point cannot be passed with a Newton-Raphson method. An indirect control algorithm (Riks, 1979) is necessary to control the computation and pass such a limit point. In a FE scheme, the iterative procedure is (Fig. 7):

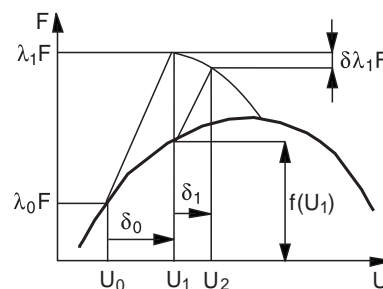


Fig. 7. Indirect control algorithm after Riks (1979)
Bild 7. Indirekter Kontroll-Algorithmus (Riks 1979)

$$\begin{cases} \mathbf{K}\delta_i = \lambda_{i+1}\mathbf{F} - \mathbf{f}(\mathbf{U}_i) \\ \lambda_{i+1} = \lambda_i + \delta\lambda_i \\ g(\delta\lambda_i) = 0 \end{cases} \quad (14)$$

Subscript i denotes the iteration, \mathbf{K} is the global stiffness matrix, \mathbf{U}_i is vector of nodal displacements, δ_i is the incremental displacement vector, \mathbf{F} is the nodal force vector, scalar λ_i denotes the reached level of force at iteration i . In the Newton-Raphson method ($\delta\lambda_i = 0$), by the indirect control method the load factor is released. It is then necessary to impose a constraint ($g(\delta\lambda_i) = 0$).

To ensure good convergence, a local constraint that considers only the more significant degrees of freedom in the increase of damage is used. It consists of imposing a constant jump of displacement between nodes α and β during iterations along the direction n ($n = 1, 2$ is the mode of principal damage). α and β are the opposite nodes close to the Gauss point where the increase of damage at the first iteration was maximum. $\delta\lambda_i$ is given by:

$$(\delta_i)_n^\alpha - (\delta_i)_n^\beta = 0 \quad \text{for } i \geq 1 \quad (15)$$

4 Numerical analysis of tests

The fracture of four TPB tests is simulated ($h = b = 45$ mm). Thus, only the mode I of fracture is considered.

The first two specimens (sp1 and sp2, tests 3 in Table 1) are made of sitka spruce with RL and TL orientations, with a density of 440 kg/m^3 and with fracture energies close to the mean experimental values ($G_{\text{FRL}} = 220 \text{ Nm/m}^2$, $G_{\text{FTL}} = 162 \text{ Nm/m}^2$). The two other ones (sp3 and sp4, tests 1 in Table 1) are made of spruce with RL and TL orientations, with a density of 400 kg/m^3 ($G_{\text{FRL}} = 174 \text{ Nm/m}^2$, $G_{\text{FTL}} = 100 \text{ Nm/m}^2$).

4.1 Determination of elastic properties of specimens

The elastic moduli were chosen in a first step according to EN338 with respect to the actual density: class C30 for sp1 and sp2 ($E_L = 12 \text{ GPa}$, $G_{LT} \cong G_{LR} = 0.75 \text{ GPa}$), class C24 for sp3 and sp4 ($E_L = 11 \text{ GPa}$, $G_{LT} \cong G_{LR} = 0.69 \text{ GPa}$). The Poisson coefficient $\nu_{\text{RL}} = \nu_{\text{TL}}$, chosen equal to 0.45, has little influence. The standard EN338 gives a mean transverse Young modulus value ($E_{90} = 1/2 (E_R + E_T)$) which did not give the correct beam stiffness. Then, E_R and E_T were determined for each couple of specimens with the global stiffness of the beam during the elastic stage of the test. Note that E_R and E_T values are of major importance compared to the influence of other elastic characteristics. It is found: $E_R = 1 \text{ GPa}$, $E_T = 0.4 \text{ GPa}$ for sp1 and sp2 specimens and $E_R = 0.53 \text{ GPa}$, $E_T = 0.3 \text{ GPa}$ for sp3 and sp4 ones.

4.2 By means of linear elastic fracture mechanics

The energy release rate $G(P, a)$ is computed by the crack closure technique. The critical energy release rate (G_c) is conventionally identified from the ultimate load of a fracture test. The initial crack length seems to have no influence on G_c for double cantilever beams specimens (Valentin and Morlier, 1982) and single end notched

specimens (Ewing and Williams, 1979). The theoretical critical energy release rate (G_c) of each specimen is determined from the maximum load ($P = P_u$) and for the initial crack length ($a = a_0 = 0.6 h$) with the equation:

$$G_c = G(P, a) \quad (16)$$

The crack propagation is then analyzed with the identified value of G_c by increasing the crack length and by applying (16). Results are given in Figs. 8–11. By comparing computational and experimental results, it appears that the LEFM approach can predict the load-displacement curve but as expected, the G_c value is very different from G_f . By assuming that the chosen elastic constants are correct, the G_c values (Figs. 8–11) are low compared with the G_f values. This result is not very surprising because G_c is related to the onset of propagation of a manufactured notch (with no process zone at the notch tip) and G_f is related to all the fracture process (i.e. essentially to the propagation of a natural crack).

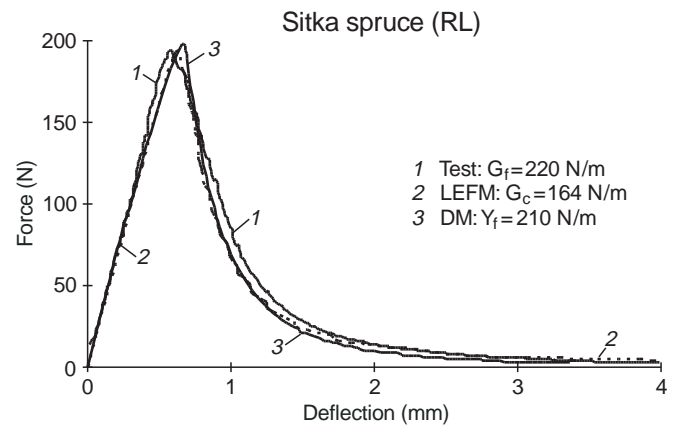


Fig. 8. Load-deflection curve for the specimen sp1 ($h = b = 45$ mm)

Bild 8. Verformung in Abhängigkeit von der Last für Probe sp1 ($h = b = 45$ mm)

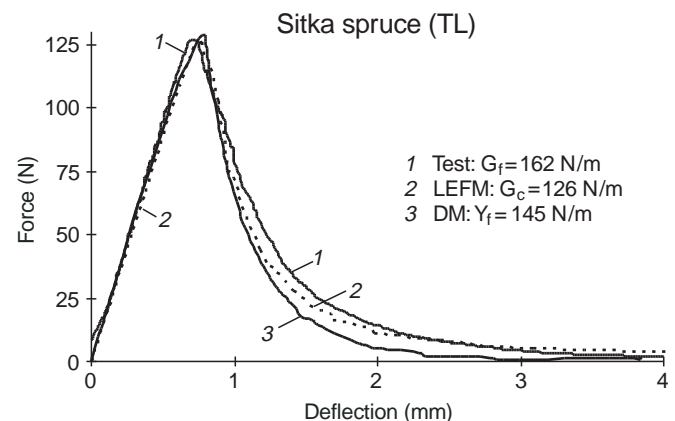


Fig. 9. Load-deflection curve for the specimen sp2 ($h = b = 45$ mm)

Bild 9. Verformung in Abhängigkeit von der Last für Probe sp2 ($h = b = 45$ mm)

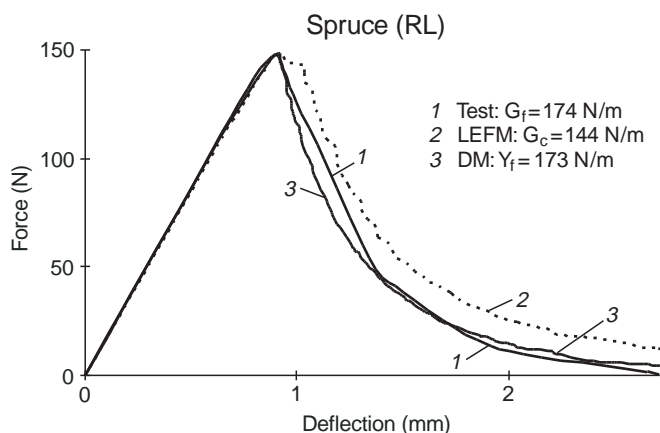


Fig. 10. Load-deflection curve for the specimen sp3 ($h = b = 45$ mm)
 Bild 10. Verformung in Abhängigkeit von der Last für Probe sp3 ($h = b = 45$ mm)

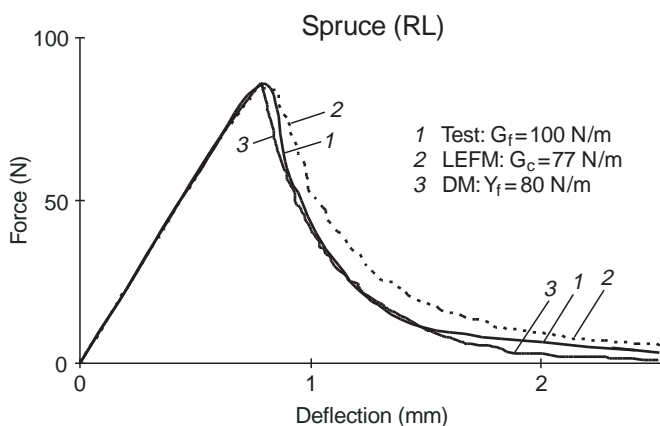


Fig. 11. Load-deflection curve for the specimen sp4 ($h = b = 45$ mm)
 Bild 11. Verformung in Abhängigkeit von der Last für Probe sp4 ($h = b = 45$ mm)

4.3 By means of damage mechanics

Cracking is now taken into account by means of joint elements in the mid-plane of the beam. The elastic constants were given. Only the characteristic parameters of the damage model (6), (7) have to be determined.

In the analysis of fracture in mode I of an already cracked structure the major parameter that governs cracking is the fracture energy Y_f , which is the area under the stress-relative displacement curve (Fig. 6). Its value is given in (10) ($c = 0$). Figure 3 shows the influence of the initial crack length on the load-deflection response for a given set of parameters. It was noticed that the curve ($a_0 = 0$) depends on the fracture energy (Y_f), the stiffness ($k = k_2$; $k_1 = 0$) and the exponent (n) but the curve ($a_0 = 0.6h$) depends essentially on Y_f . That remark confirms that the fracture energy (Y_f) is the parameter that governs fracture propagation. Notice on Fig. 3 the snap-back curve for short cracks which justifies the presented

indirect control algorithm. In this paper, only the propagation of an existing crack is studied. According to the previous remark, k and n can be chosen very roughly. Nevertheless, a tentative identification procedure of these parameters is proposed. $[u]_c$ is defined as the critical crack tip opening displacement such that the continuum has no cohesion (Fig. 6):

$$[u]_c = \sqrt{\frac{2(n+1)Y_f}{nk}} \quad (17)$$

For a given Y_f , as k or n grows, the ductility ($[u]_c$) decreases. Thus it seems necessary to introduce in the model a characteristic length that characterizes the process zone length and therefore the brittleness. Such characteristic lengths were introduced by Irwin (1957) in fracture mechanics of metallic materials with confined plasticity or Hillerborg et al., (1976), Bazant et al. (1987, 1990) for concrete, Gustafsson (1985, 1988) for wood. All these characteristic lengths (or brittleness numbers) are substantially equivalent in the description of size effects and the associated transition from ductile behavior to brittle LEFM behavior.

Examine the specimen sp1 in Fig. 8. In order to estimate the unknown parameters, the following assumptions concerning the transverse tensile strength ($f_{t,90}$), the fracture energy (Y_f) and the exponent (n) are chosen:

$$f_{t,90} = 4.5 \text{ MPa}; \quad Y_f = G_f = 220 \text{ Nm/m}^2; \quad n = 0.2 \quad (18)$$

Then, the only unknown parameter (k) is identified such that the maximum stress is equal to $f_{t,90}$, which gives:

$$k = 500 \text{ N/mm}^3 \quad (19)$$

It was verified numerically that the identified value of k is not too low and does not affect the global beam stiffness. The choice of the n value is justified by the value of the critical crack tip opening displacement (17):

$$[u]_c = 0.08 \text{ mm} \quad (20)$$

This value is close to the one proposed by Gustafsson (1985) (0.2 mm). This value is very small and may explain that LEFM is valid for the large specimens investigated ($h = 67, 100$ mm) in which the process zone length may be neglected.

Previous k and n values are kept constant for the four considered simulations. Like in LEFM, the fracture energy Y_f is determined from ultimate loads. Figures 8–11 give the Y_f values and the load-deflection curves obtained from tests and from LEFM and DM simulations.

Load-displacement curves are correctly described by the DM approach. The major point is that for the RL wood orientation, the experimental fracture energy (G_f) value is very close to the fracture energy value used in the modeling (Y_f). There is a slight difference between G_f and Y_f in the case of the TL orientation certainly due to the uncertainty in the identification of elastic stiffnesses and damage parameters.

Conclusions

5.1

Experiments

The CIB-W18 draft standard for fracture energy determination is a simple method to obtain the fracture energy G_f of wood in tension perpendicular to the grain.

A sharp notch finalized with a razor blade and an initial crack length equal to 60% of the beam depth ensures stable load-deflection curves.

The size effect study shows that LEFM is not valid for the 45 mm specimen analysis. An important result is that the fracture energy is not size dependent.

5.2

Numerical analysis of tests

An interface model based on Damage Mechanics has been presented for the analysis of cracking under pure or mixed mode conditions in an orthotropic medium such as wood. A link between DM parameters and LEFM parameters allows a clear identification of the parameters of the model. The use of joint elements to simulate the crack propagation is easy to implement in a FE code.

Only pure mode I conditions were examined numerically. Comparisons between simulation results with LEFM and experimental results of the TPB test have shown that LEFM could predict the load-displacement curve but the critical energy release rate could not be chosen equal to the fracture energy. This is due to non-linear phenomena which occur in the process zone.

The load-deflection curve is correctly predicted by the DM model. In addition, it was shown that the fracture energy was the major parameter that governs fracture propagation in linear (large structures) or in non-linear (small structures) fracture studies.

References

- Aicher S (1992) Fracture energies and size effect law for spruce and oak in mode I, Determination of fracture properties of wood especially in mode II and mixed modes I and II. Proceedings of the RILEM TC 133 Meeting, Bordeaux France
- Aicher S, Reinhardt HW, Klöck W (1993) Nichtlineares bruchmechanik-maßstabsgesetz für fichte bei zugbeanspruchung senkrecht zur faserichtung. Holz als Roh- und Werkstoff 51: 385-394
- Allix O, Daudeville L, Neau JL, Ladevèze P (1995) Necessity of using damage mechanics for the analysis of delamination specimens. 4th Int. Conf. on Computational Plasticity COMPLAS IV, Barcelona Spain
- Bazant ZP (1984) Size effect in blunt fracture: concrete, rock, metal. J. Eng. Mechanics 104: 518-535
- Bazant ZP, Kazemi MT (1990) Determination of fracture energy, process zone, length and brittleness number from size effect, with application to rock and concrete. Int. J. Fracture 44(2): 111-131
- Bazant ZP, Pfeiffer PA (1987) Determination of fracture energy from size effect and brittleness number. ACI Mat. J. 85: 463-480
- Boström L (1988) The fictitious crack model - A fracture mechanics approach applied on wood. International Conference on Timber Engineering, Seattle DC, 2: 559-565
- Ewing PD, Williams JG (1979) Thickness and moisture content effect in the fracture toughness of Scots Pine. J. Mat. Sci. 14-12: 2959-2966
- Garcia-Alvarez VO, Carol I, Gettu R (1994) Numerical simulation of fracture in concrete using joint elements. Anales de Mecanica de la Fractura 11: 75-80
- Gens A, Carol I, Alonso EE (1988) An interface element formulation for the analysis of soil-reinforcement interaction. Comp. Geotechnics 7: 133-151
- Griffith A (1920) The phenomena of rupture and flow in solids. Philosophical Transactions of the Royal Society of London. Series A. 221: 163-198
- Gustafsson PJ (1988) A study of strength of notched beams. 21th CIB-W18 meeting. Vancouver Canada. Paper 21-10-1
- Gustafsson PJ (1985) Fracture mechanics studies of non-yielding materials like concrete. Technical Report TVBM-1007. Lund Institute of Technology Sweden
- Hillerborg A, Modeer M, Petersson PE (1976) Analysis of crack formation and crack growth in concrete by means of fracture mechanics and finite elements. Cement and Concrete Research 6: 773-782
- Hohberg JM, Bachmann H (1988) A macro joint element for non-linear arch dam analysis. Numerical Methods in Geomechanics, Ed. Swoboda G, Balkema, Rotterdam, 829-834
- Hunt DG, Croager WP (1982) Mode II fracture toughness of wood measured by a mixed mode test method. J. Mat. Sci. Letters 1: 77-79
- Irwin GR (1957) Analysis of stresses and strains near the end of a crack transversing a plate. ASME J. Appl. Mech. Transactions 24(3): 361-364
- Jenq YS, Shah SP (1985) A two parameter fracture model for concrete. J. Eng. Mech. 111(4): 1227-1241
- Larsen HJ, Gustafsson PJ (1989) Design of end-notched beams. 22th CIB-W18 A meeting. Berlin Germany. Paper 22-10-1
- Larsen HJ, Gustafsson PJ (1990) The fracture energy of wood in tension perpendicular to the grain. 23th CIB-W18 A meeting. Lisbon Portugal. Paper 23-19-2
- Lum C, Foschi O (1988) Arbitrary V-notches in orthotropic plates, J. Eng. Mech. 114(4): 638-655
- Mall S, Murphy JF, Shottafer JE (1983) Criterion for mixed mode fracture in wood. J. Eng. Mech. 109(3): 680-690
- Murphy JF (1986) Strength and stiffness reduction of large notched beams. J. Struct. Eng. 112(9): 1989-2000
- Nallathambi P, Karihaloo BL (1986) Determination of specimen-size independent fracture toughness of plain concrete. Magazine of Concrete Research 38(135): 67-76
- Ngo D, Scordelis AC (1967) Finite element analysis of reinforced concrete beams. J. the American Concrete Institute 64(14): 152-163
- Patton-Mallory M, Cramer SM (1987) Fracture mechanics: a tool for predicting wood component strength. Forest Products Journal 37(7-8): 39-47
- Riks E (1979) An incremental approach to the solution of snapping and buckling problems. Int. J. Solids and Structures 15: 524-551
- Rots JG, Schellekens JCJ (1990) Interface elements in concrete mechanics. 2nd Int. Conf. on Computer Aided Analysis and Design of Concrete Structures SCI-C, Volume 2
- Triboulot P, Jodin P, Pluvinage G (1984) Validity of fracture mechanics concepts applied to wood and finite element calculation. Wood Sci. Tech. 18(61): 11-24
- Valentin G, Boström L, Gustafsson PJ, Ranta-Maunus A, Gowda S (1991) Application of fracture mechanics to timber structures. RILEM state-of-art Report. Technical Research Centre of Finland, Espoo, Research Notes 1262
- Valentin G, Morlier P (1982) A criterion of crack propagation in timber. Materials and Structures 15: 88-95
- Wu EM (1967) Application of fracture mechanics to anisotropic plates. J. Appl. Mech. Series E 34(4): 967-974